A comparison between chip fractional and non fractional sampling for a direct sequence CDMA receiver

François Horlin, L. Vandendorpe
Communications and Remote Sensing Laboratory, Université catholique de Louvain,
Place du Levant, 2 - 1348 Louvain-la-Neuve, Belgium,
{*horlin,vandendorpe*}*@tele.ucl.ac.be*

Abstract— **This paper examines the effects of chip fractional (CF) and chip non fractional (CNF) sampling on the performance of a CDMA uplink receiver. The impact of the receiver front end filter, which is sampling rate dependent, is investigated. Models for burst and continuous transmissions are introduced. The discrete time equivalent channels between the various users and the receiver are assumed to be known. Firstly, the mutual information between the emitted sequences of symbols and the received sequence is investigated. It is analytically shown that the receiver loses systematically information in case of CNF sampling. Secondly, we have demonstrated that the CF receiver always achieves better performance in term of minimum mean square error (MMSE) for both linear and decision feedback (DF) structures. A closed form expression of the gain in performance is provided for the two metrics under consideration. The importance of the gain due to CF sampling is also illustrated by means of computations for multi-path channels. For a typical system setup, a gain of 0.1 bits per emitted symbol is observed for the mutual information. Considering the geometrical mean of symbol SINRs in case of linear and DF joint detection (JD) for a roll-off factor equal to 0.3, a gain of 0.4 dB arises for the CF linear detector and a gain of 0.2 dB arises for the CF DF detector.**

I. Introduction

Direct sequence code division multiple access (DS-CDMA) is a multi-user transmission technique that became very popular these recent years. Several features make this multiple access technique attractive for communications in wireless cellular networks. Firstly DS-CDMA is a wide-band transmission technique. When the bandwidth is large enough, it is possible to benefit from multi-path propagation mechanisms. Secondly the physical resource is the code and no longer the time or the frequency. Together with the capability of DS-CDMA to use the information carried by several replicas of the same signal this feature is also the key for soft hand-over [18]. Next, in the uplink, no synchronism between users is required. As a matter of fact, if the codes allocated to different active users are properly designed, the cross-correlations will be small and the interference due to the other users can be seen as additional background noise.

With respect to these ideal expectations, there are however a number of limitations. First of all, rake receivers which are able to combine the information carried by different paths, are only optimum with respect to background noise. They do not solve inter-symbol interferences (ISI) or multiple-access interferences (MAI). A related problem is that if other users are handled as additional background noise and if only single user receivers are used, the number of users that can be accommodated by the system is strongly limited.

This has lead quite soon to the investigation and the design of more efficient receiver structures. Verdu has published in [6] the structure of the optimum multi-user receiver for asynchronous Gaussian channels. It is made up of a bank of matched filters followed by a Viterbi detector. As this algorithm has a complexity exponential in the number of users, a lot of effort has been devoted to the design of sub-optimum yet of acceptable complexity receivers. A very good overview can be found in [19]. Similarly to the equalizers used to counteract ISI channels, there are linear and decision-feedback (DF) multi-user detectors. Furthermore they can be designed for a zero-forcing (ZF) or a minimum mean square error (MMSE) criterion. The decorrelating detector reported in [7] is basically a linear ZF detector. Linear and DF MMSE receivers have been reported by Duel-Hallen in [8, 9]. As for burst transmission, linear and DF solutions designed for both a ZF or an MMSE criterion are reported in [13, 14].

On another hand much attention is presently paid to fully digital receivers [21]. Meyr has investigated in [2] the conditions on the sampling rate and on the analog prefilter such that the samples of a band-limited signal represent sufficient statistics. The performance of fractionally spaced equalizer (FSE) is studied in [4] for single user transmission. It is shown that if the sampling rate of the received signal (more precisely the useful part of the received signal, not the noise) is in accordance with Shannon sampling theorem, an infinite FSE has the potential of the optimum linear receiver. A good overview of FSE receivers can be found in [3].

In the early implementations, DS spreading was usually applied as a multiplication after the modulation and the spectrum of the transmitted signal was indeed very large. In recent DS-CDMA systems, the spreading operation is implemented as an interpolation of the information symbols and the signal resulting from this operation still enters a shaping filter. If the chip period is denoted by T_c and if a half-root Nyquist filter is used for the shaping, the transmitted signal has a spectrum upper limited to $0.5 \times (1+\eta)/T_c$ where η is the roll-off factor. Hence a sampling rate of $2/T_c$ is sufficient. However in a number of contributions, sampling of the received signal at $1/T_c$ is assumed : for instance, [13, 14].

In [5] the authors analyze the performance of fractionally chip sampled linear multi-user detectors. An ideal low-pass (LP) filter is applied on the received signal in order to avoid aliasing. They consider an asynchronous DS-CDMA system with frequency selective channels. They show that fractionally spaced receivers of sufficient length satisfy a necessary condition for the existence of ZF solutions under conditions where no finite impulse response (FIR) solution exists for non fractionally spaced receivers. Furthermore simulation results are provided which indicate that for sufficient lengths, fractionally spaced receivers may achieve better MMSE performance than non fractional ones in the presence of additive white Gaussian noise (AWGN).

The purpose of the present paper is to investigate the performance of $2/T_c$ and $1/T_c$ receivers. These configurations will be named chip fractional (CF) and chip non fractional (CNF). The investigations will be carried out for linear and DF receivers and for both burst and continuous transmission schemes. Two performance measures will be used: the mutual information between the emitted symbol sequences and the received one, and the variance of estimation errors. Assuming that the first element of the receiver (after conversion to baseband) is a perfect LP presampling filter which limits the spectrum in accordance with the subsequent sampling rate ($0.5/T_c$ for CNF and $1/T_c$ for CF receivers), we will demonstrate that CF receivers outperform CNF ones and quantify the gain in performance. In short, we investigate the benefit related to the processing of the spectral information above $0.5/T_c$. Figures for the performance difference will also be provided by means of computations. In order to be complete, the case where the receiver front end is a chip matched filter (MF) followed by chip rate sampling is also considered in the computational results.

The paper is organized as follows. In the first part, burst transmission is assumed. A CF model is proposed in which the CNF situation can easily be isolated and used as a reference. As a result, one derives for the CF situation mutual information and symbol estimation error variance (for the linear and DF MMSE joint detectors) expressions in which the CNF counterpart is easily identified. In the second part, the same steps are followed for the case of continuous transmission.

In the following sections, the symbols $(.)^*$, $(.)^T$, $(.)^H$ will be used to denote the complex conjugate, the transpose and the complex conjugate transpose respectively of a matrix, or a vector, or a scalar. Notation $|.|$ stands for the determinant of a matrix.

II. System model

We assume an asynchronous multi-user DS-CDMA uplink where each user transmits information over a frequency selective channel. A model of the transmission system is given in Figure 1. Each active user k transmits a sequence of symbols $d_k(n)$ at baud-rate $1/T$ ($k = 1, \cdots, K$). The symbol sequence is spread by the code sequence $s_k(n)$ and shaped with the chip shaping filter $u(t)$ (half-root Nyquist). T_c is the chip duration and N_c is the spreading factor. Each user signal is transmitted over a user specific frequency selective channel with low-pass impulse response $c_k(t)$. Function $p(t)$ represents the receiver sampling prefilter, supposed to be an ideal presampling LP filter. For a T_c/M spaced detector, the cutoff frequency is $0.5\,M/T_c$. We define the composite impulse responses $h_k(t) \stackrel{def}{=} u(t) \otimes c_k(t) \otimes p(t)$. The operator $\otimes$ represents the convolution. $w(t)$ is the additive noise (an AWGN is often a sufficient model). As the received signal is sampled at a rate $1/T_s = M/T_c = MN_c/T$, we get the following discrete time model

$$r(m) = \sum_{k=1}^{K} \sum_{n=-\infty}^{\infty} d_k(n)\, g_k(m - nMN_c) + v(m) \quad (1)$$

where $r(m)$ is the received sequence and $v(m)$ is the noise sequence obtained after receiver filtering and sampling. The discrete time equivalent total impulse responses which include the user codes, the chip shaping filters, the user channels and the receiver prefilter, are denoted by $g_k(n)$.

III. Burst transmission

A. System decomposition

To be able to compare the CF ($M = 2$) and CNF ($M = 1$) detectors, the information processed by the CF receiver is organized in such a way that a subset corresponds to the information available to the CNF receiver. This is done first by separating the frequency content below and above $0.5/T_c$, and then by using polyphase components.

Firstly, the receiver prefilter is separated in two parts in the frequency domain (see Figure 2)

$$P(f) = P^{\alpha}(f) + P^{\beta}(f)$$

where $P^{\alpha}(f)$ corresponds to the prefilter applied before a CNF sampling and $P^{\beta}(f)$ is the added part in case of CF sampling. $P(f)$, $P^{\alpha}(f)$ and $P^{\beta}(f)$ are the Fourier transforms of $p(t)$, $p^{\alpha}(t)$ and $p^{\beta}(t)$. We note $g_k^{\alpha}(n)$ and $g_k^{\beta}(n)$, the separated discrete time equivalent total impulse responses including each of the prefilter parts and obtained after a CF sampling for each user k. $G_k^{\alpha}(e^{j\Omega})$ and $G_k^{\beta}(e^{j\Omega})$ denote their Fourier transforms.

Secondly, a separation of even and odd samples of the received signal is introduced. In the following notations, index "0" corresponds to the even samples or polyphase component 0, and index "1" corresponds to odd samples or polyphase component 1. Let us define

$$r^i(n) \stackrel{def}{=} r(2n+i) \quad (2)$$

$$v^i(n) \stackrel{def}{=} v(2n+i) \quad (3)$$

$$g_k^{i,\gamma}(n) \stackrel{def}{=} g_k^{\gamma}(2n+i) \quad (4)$$

for $\gamma = \alpha, \beta$ and $i = 0, 1$. $G_k^{i,\gamma}(e^{j\Omega})$ denotes the Fourier transform of the sequence $g_k^{i,\gamma}(n)$. It can be related to

$G_k^{\gamma}(e^{j\Omega})$ by the use of the properties of the polyphase components [22]. We have

$$G_k^{i,\gamma}(e^{j\Omega}) = \frac{1}{2} e^{\frac{ji\Omega}{2}} \left[G_k^{\gamma}(e^{\frac{j\Omega}{2}}) + (-1)^i G_k^{\gamma}(e^{\frac{j(\Omega-2\pi)}{2}}) \right]. \quad (5)$$

In case of burst transmission, each user sends a packet of N symbols. There is a guard time between successive bursts that should be long enough to prevent inter-burst interferences. If we consider that the received signal is sampled at CF rate, we get the following observation model

$$\begin{aligned} \boldsymbol{r}^{CF} &\stackrel{def}{=} \begin{bmatrix} \boldsymbol{r}^0 \\ \boldsymbol{r}^1 \end{bmatrix} \\ &= \begin{bmatrix} \boldsymbol{G}^{0,\alpha} + \boldsymbol{G}^{0,\beta} \\ \boldsymbol{G}^{1,\alpha} + \boldsymbol{G}^{1,\beta} \end{bmatrix} \boldsymbol{d} + \begin{bmatrix} \boldsymbol{v}^0 \\ \boldsymbol{v}^1 \end{bmatrix} \\ &\stackrel{def}{=} \boldsymbol{G}^{CF}\,\boldsymbol{d} + \boldsymbol{v}^{CF} \end{aligned} \quad (6)$$

with

$$\boldsymbol{d} \stackrel{def}{=} \begin{bmatrix} \boldsymbol{d}_1 \\ \vdots \\ \boldsymbol{d}_K \end{bmatrix} \quad \text{and} \quad \boldsymbol{d}_k \stackrel{def}{=} \begin{bmatrix} d_k(0) \\ \vdots \\ d_k(N-1) \end{bmatrix}$$

$$\boldsymbol{r}^i \stackrel{def}{=} \begin{bmatrix} r^i(0) \\ \vdots \\ r^i(NN_c + L - 1) \end{bmatrix}$$

$$\boldsymbol{v}^i \stackrel{def}{=} \begin{bmatrix} v^i(0) \\ \vdots \\ v^i(NN_c + L - 1) \end{bmatrix}.$$

L denotes the length of the impulse responses $h_k(t)$, evaluated in chip periods. Furthermore, the matrices $\boldsymbol{G}^{i,\gamma}$ are defined in Figure 3. They are respectively made of delayed versions of the following vectors

$$\boldsymbol{g}_k^{i,\gamma} \stackrel{def}{=} \begin{bmatrix} g_k^{i,\gamma}(0) \\ g_k^{i,\gamma}(1) \\ \vdots \\ g_k^{i,\gamma}(N_c + L - 1) \end{bmatrix}.$$

In case of CNF sampling ($M = 1$), the model reduces to

$$\boldsymbol{r}^{CNF} = \boldsymbol{G}^{CNF}\,\boldsymbol{d} + \boldsymbol{v}^{CNF} \quad (7)$$

where matrix $\boldsymbol{G}^{CNF}$ is equal to $\boldsymbol{G}^{0,\alpha}$.

B. Matrices expansion

If an AWGN is assumed, each performance measure (mutual information or error variance) is a function of $(\boldsymbol{G}^{CF})^H \boldsymbol{G}^{CF}$ in case of CF sampling and of $(\boldsymbol{G}^{CNF})^H \boldsymbol{G}^{CNF}$ in case of CNF sampling. Furthermore $\boldsymbol{G}^{CNF} = \boldsymbol{G}^{0,\alpha}$ (see equality (7)). For CF sampling, it is possible to rewrite the last expressions using the definition of $\boldsymbol{G}^{CF}$ (see equality (6)). This leads to

$$\begin{aligned} (\boldsymbol{G}^{CF})^H \boldsymbol{G}^{CF} &= (\boldsymbol{G}^{0,\alpha})^H \boldsymbol{G}^{0,\alpha} + (\boldsymbol{G}^{1,\alpha})^H \boldsymbol{G}^{1,\alpha} \\ &+ (\boldsymbol{G}^{0,\beta})^H \boldsymbol{G}^{0,\beta} + (\boldsymbol{G}^{1,\beta})^H \boldsymbol{G}^{1,\beta} \\ &+ (\boldsymbol{G}^{0,\alpha})^H \boldsymbol{G}^{0,\beta} + (\boldsymbol{G}^{1,\alpha})^H \boldsymbol{G}^{1,\beta} \\ &+ (\boldsymbol{G}^{0,\beta})^H \boldsymbol{G}^{0,\alpha} + (\boldsymbol{G}^{1,\beta})^H \boldsymbol{G}^{1,\alpha}. \end{aligned} \quad (8)$$

Each term of this last expression can be expanded. For example, consider matrix $(\boldsymbol{G}^{0,\alpha})^H \boldsymbol{G}^{0,\alpha}$ (first term of equation (8)). According to the different user parts $\boldsymbol{G}_k^{0,\alpha}$ that constitute matrix $\boldsymbol{G}^{0,\alpha}$ (see Figure 3), the product $(\boldsymbol{G}^{0,\alpha})^H \boldsymbol{G}^{0,\alpha}$ can be written as

$$(\boldsymbol{G}^{0,\alpha})^H \boldsymbol{G}^{0,\alpha} = \begin{bmatrix} (\boldsymbol{G}_1^{0,\alpha})^H \boldsymbol{G}_1^{0,\alpha} & \cdots & (\boldsymbol{G}_1^{0,\alpha})^H \boldsymbol{G}_K^{0,\alpha} \\ \vdots & \ddots & \vdots \\ (\boldsymbol{G}_K^{0,\alpha})^H \boldsymbol{G}_1^{0,\alpha} & \cdots & (\boldsymbol{G}_K^{0,\alpha})^H \boldsymbol{G}_K^{0,\alpha} \end{bmatrix}.$$

Each submatrix $(\boldsymbol{G}_k^{0,\alpha})^H \boldsymbol{G}_l^{0,\alpha}$ $(k,l = 1,\cdots,K)$ is a Toeplitz matrix of size N generated [1] by the sequence

$$\begin{aligned} & x_{kl}^{0,\alpha;0,\alpha}(m) \\ &= \sum_{n=-\infty}^{\infty} g_l^{0,\alpha}(n) \left(g_k^{0,\alpha}(n - mN_c) \right)^* \quad (9) \\ &= \frac{1}{2\pi} \int_{-\pi}^{\pi} G_l^{0,\alpha}(e^{j\Omega}) \left(G_k^{0,\alpha}(e^{j\Omega}) \right)^* e^{-jmN_c\Omega}\, d\Omega \quad (10) \\ &= \frac{1}{8\pi} \int_{-\pi}^{\pi} G_l^{\alpha}(e^{j\frac{\Omega}{2}}) \left(G_k^{\alpha}(e^{j\frac{\Omega}{2}}) \right)^* e^{-jmN_c\Omega}\, d\Omega \\ &+ \frac{1}{8\pi} \int_{-\pi}^{\pi} G_l^{\alpha}(e^{j\frac{\Omega-2\pi}{2}}) \left(G_k^{\alpha}(e^{j\frac{\Omega-2\pi}{2}}) \right)^* e^{-jmN_c\Omega}\, d\Omega \quad (11) \end{aligned}$$

where equality (10) comes from the Parseval relation. Equality (11) can be obtained by using property (5) of the polyphase components and by noting that there is no spectral overlap between $G_l^{\alpha}(e^{j\frac{\Omega}{2}})$ and $G_k^{\alpha}(e^{j\frac{\Omega-2\pi}{2}})$ nor between $G_l^{\alpha}(e^{j\frac{\Omega-2\pi}{2}})$ and $G_k^{\alpha}(e^{j\frac{\Omega}{2}})$ which makes the corresponding products $G_l^{\alpha}(e^{j\frac{\Omega}{2}}) \left(G_k^{\alpha}(e^{j\frac{\Omega-2\pi}{2}} \right)^*$ and $G_l^{\alpha}(e^{j\frac{\Omega-2\pi}{2}}) \left(G_k^{\alpha}(e^{j\frac{\Omega}{2}}) \right)^*$ equal to 0.

The second term of equality (8) is matrix $(\boldsymbol{G}^{1,\alpha})^H \boldsymbol{G}^{1,\alpha}$. It is made of a set of submatrices $(\boldsymbol{G}_k^{1,\alpha})^H \boldsymbol{G}_l^{1,\alpha}$ $(k,l = 1,\cdots,K)$ corresponding to the different users. Each submatrix is a Toeplitz matrix generated by the sequence

$$\begin{aligned} & x_{kl}^{1,\alpha;1,\alpha}(m) \\ &= \frac{1}{8\pi} \int_{-\pi}^{\pi} G_l^{\alpha}(e^{j\frac{\Omega}{2}}) \left(G_k^{\alpha}(e^{j\frac{\Omega}{2}}) \right)^* e^{-jmN_c\Omega}\, d\Omega \\ &+ \frac{1}{8\pi} \int_{-\pi}^{\pi} G_l^{\alpha}(e^{j\frac{\Omega-2\pi}{2}}) \left(G_k^{\alpha}(e^{j\frac{\Omega-2\pi}{2}}) \right)^* e^{-jmN_c\Omega}\, d\Omega \end{aligned} \quad (12)$$

[1] $[\boldsymbol{G}_k^H \boldsymbol{G}_l]_{mn} = x_{kl}(m-n)$ for $m,n = 0,\cdots,N-1$

where the same developments were applied as in equality (11).

A comparison between equalities (11) and (12) shows that

$$(\boldsymbol{G}^{0,\alpha})^H \boldsymbol{G}^{0,\alpha} = (\boldsymbol{G}^{1,\alpha})^H \boldsymbol{G}^{1,\alpha} \quad (13)$$

(the respective products of the submatrices are Toeplitz matrices generated by identical sequences).

The following results can be obtained by using similar steps:

$$\begin{aligned} (\boldsymbol{G}^{0,\beta})^H \boldsymbol{G}^{0,\beta} &= (\boldsymbol{G}^{1,\beta})^H \boldsymbol{G}^{1,\beta} && (14)\\ (\boldsymbol{G}^{0,\alpha})^H \boldsymbol{G}^{0,\beta} &+ (\boldsymbol{G}^{1,\alpha})^H \boldsymbol{G}^{1,\beta} = \boldsymbol{0}_{KN} && (15)\\ (\boldsymbol{G}^{0,\beta})^H \boldsymbol{G}^{0,\alpha} &+ (\boldsymbol{G}^{1,\beta})^H \boldsymbol{G}^{1,\alpha} = \boldsymbol{0}_{KN}\,. && (16) \end{aligned}$$

Finally, from equalities (8), (13), (14), (15) and (16), we have

$$(\boldsymbol{G}^{CF})^H \boldsymbol{G}^{CF} = 2\left[(\boldsymbol{G}^{0,\alpha})^H \boldsymbol{G}^{0,\alpha} + (\boldsymbol{G}^{0,\beta})^H \boldsymbol{G}^{0,\beta}\right]. \quad (17)$$

The first term corresponds to the CNF detector and the second term is the additional information available in case of CF sampling. Remember that the noise variance in case of CF joint detector $(\sigma_v^{CF})^2$ is twice the noise variance in case of CNF joint detector $(\sigma_v^{CNF})^2$. This is due to the different bandwidths of the ideal presampling filters. In practice the channel impulse responses (CIRs) are either time or frequency limited. The demonstration approximates this fact assuming that the CIRs are of sufficient length to be also highly frequency band-limited.

Cross-correlation between two vectors in a burst transmission scheme is defined as $\boldsymbol{R}_{xy} = E\left[\boldsymbol{x}\,\boldsymbol{y}^H\right]$ where $E[]$ denotes the expectation operator. We define the following matrices

$$\begin{aligned} \boldsymbol{P} &\stackrel{def}{=} \left[\boldsymbol{R}_{dd}^{-1} + \frac{1}{(\sigma_v^{CNF})^2}(\boldsymbol{G}^{0,\alpha})^H \boldsymbol{G}^{0,\alpha}\right]^{-1} && (18)\\ \boldsymbol{Q} &\stackrel{def}{=} (\boldsymbol{G}^{0,\beta})^H && (19)\\ \boldsymbol{T} &\stackrel{def}{=} (\sigma_v^{CNF})^2\,\boldsymbol{I}_{NN_c+L-1} && (20) \end{aligned}$$

in order to simplify the expressions in sections III-C, III-D and III-E. Matrix $\boldsymbol{I}_{NN_c+L-1}$ is the identity matrix of size NN_c+L-1.

C. Mutual information

If an AWGN of variance $(\sigma_v^{CF})^2$ and Gaussian independent symbols of variance σ_d^2 are assumed, the mutual information between the vector of emitted symbols and the received vector is given, in case of CF sampling, by

$$\begin{aligned} & I(\boldsymbol{d};\boldsymbol{r}^{CF}) \\ &= \log\left|\boldsymbol{I}_{KN} + \frac{\sigma_d^2}{(\sigma_v^{CF})^2}(\boldsymbol{G}^{CF})^H \boldsymbol{G}^{CF}\right| && (21)\\ &= \log\left|\boldsymbol{I}_{KN} + \frac{\sigma_d^2}{(\sigma_v^{CNF})^2}(\boldsymbol{G}^{0,\alpha})^H \boldsymbol{G}^{0,\alpha}\right| \\ &+ \log\left|\boldsymbol{I}_{KN} + \frac{1}{(\sigma_v^{CNF})^2}\boldsymbol{P}\,\boldsymbol{Q}\,\boldsymbol{Q}^H\right| && (22)\\ &= I(\boldsymbol{d};\boldsymbol{r}^{CNF}) + \log\left|\boldsymbol{I}_{KN} + \frac{1}{(\sigma_v^{CNF})^2}\boldsymbol{P}\,\boldsymbol{Q}\,\boldsymbol{Q}^H\right| \\ &. && (23) \end{aligned}$$

Equality (21) is the classical result giving the mutual information between a vector of emitted symbols and the received vector (see theorem 1 in [15]). Equality (22) comes from the expansion (17) and from the fact that the noise variance in case of CF sampling is twice the noise variance in case of CNF sampling. Definitions (18) and (19) are also used. The mutual information in case of CNF sampling appears in equality (23) (remember that $\boldsymbol{G}^{CNF} = \boldsymbol{G}^{0,\alpha}$).

In order to show that the mutual information after CF sampling is larger than the mutual information after CNF one, it is sufficient to prove that matrix $\boldsymbol{P}\,\boldsymbol{Q}\,\boldsymbol{Q}^H$ is positive definite. The following statements can be deduced from [25]:

1. If a matrix $\boldsymbol{M}_1$ is positive definite, then the matrix $\boldsymbol{M}_2^H\,\boldsymbol{M}_1\,\boldsymbol{M}_2$ is a positive definite matrix for any full column rank matrix $\boldsymbol{M}_2$.
2. The sum of two positive definite matrices is a positive definite matrix.
3. The inverse of a positive definite matrix is a positive definite matrix.

With statement 1, matrix $(\boldsymbol{G}^{0,\alpha})^H \boldsymbol{G}^{0,\alpha}$ is positive definite. With statements 2 and 3, matrix $\boldsymbol{P}$ is positive definite. Due to statement 1, matrix $\boldsymbol{P}\,\boldsymbol{Q}\,\boldsymbol{Q}^H$ is also positive definite. Hence its eigen-values are positive so that the eigen-values of $\boldsymbol{I}_{KN} + \frac{1}{(\sigma_v^{CNF})^2}\boldsymbol{P}\,\boldsymbol{Q}\,\boldsymbol{Q}^H$ are larger than "1". The determinant of a matrix is equal to the product of its eigen-values. It follows that the mutual information is always larger in case of CF sampling than in case of CNF sampling. A similar result will be obtained for the continuous transmission case and for this case, additional comments are provided in Appendix B.

D. Linear MMSE joint detector

It will be demonstrated that the symbol estimation error variances after a linear MMSE joint detector are smaller in case of CF sampling than in case of CNF sampling. We develop the error correlation matrix in the two cases and compare the diagonal elements. After CF linear MMSE joint detection (JD), the error ε auto-correlation matrix is (an AWGN of variance $(\sigma_v^{CF})^2$ is assumed)

$$\begin{aligned} & \boldsymbol{R}_{\varepsilon\varepsilon}^{CF} \\ &= \left[\boldsymbol{R}_{dd}^{-1} + \frac{1}{(\sigma_v^{CF})^2}(\boldsymbol{G}^{CF})^H \boldsymbol{G}^{CF}\right]^{-1} && (24)\\ &= \left[\boldsymbol{R}_{dd}^{-1} + \frac{1}{(\sigma_v^{CNF})^2}(\boldsymbol{G}^{0,\alpha})^H \boldsymbol{G}^{0,\alpha}\right]^{-1} \\ &- \boldsymbol{P}\,\boldsymbol{Q}\left(\boldsymbol{T} + \boldsymbol{Q}^H\,\boldsymbol{P}\,\boldsymbol{Q}\right)^{-1}\boldsymbol{Q}^H\,\boldsymbol{P} && (25)\\ &= \boldsymbol{R}_{\varepsilon\varepsilon}^{CNF} - \boldsymbol{P}\,\boldsymbol{Q}\left(\boldsymbol{T} + \boldsymbol{Q}^H\,\boldsymbol{P}\,\boldsymbol{Q}\right)^{-1}\boldsymbol{Q}^H\,\boldsymbol{P}. && (26) \end{aligned}$$

The first equality (24) is the classical expression of the error auto-correlation matrix after MMSE linear JD [14]. Equality (25) comes from expansion (17) and from the fact that the noise variance in case of CF sampling is twice the noise variance in case of CNF sampling. Equality (25) is obtained by the use of the inversion lemma [2]. Definitions (18), (19) and (20) are also used. The CNF error auto-correlation matrix appears (remember that matrix $\boldsymbol{G}^{CNF} = \boldsymbol{G}^{0,\alpha}$).

In order to show that the error variances of the CF linear MMSE detector are lower than those of the CNF linear MMSE detector, it is sufficient to prove that the second term in equality (26) is a positive definite matrix. It was demonstrated in section III-C that matrix $\boldsymbol{P}$ is positive definite. By the use of the same steps, it can be also easily demonstrated that matrix $\boldsymbol{P}\boldsymbol{Q}\left(\boldsymbol{T}+\boldsymbol{Q}^H\boldsymbol{P}\boldsymbol{Q}\right)^{-1}\boldsymbol{Q}^H\boldsymbol{P}$ is positive definite and hence, has positive diagonal elements. The symbol error variances given by the diagonal elements of the error auto-correlation matrix are thus always smaller in case of CF sampling.

E. Decision feedback MMSE joint detector

In case of DF JD, the error variances of symbol estimates are given by the diagonal elements after a Choleski decomposition of the error auto-correlation matrix obtained after pure linear JD [14]. This result accounts for the fact that previous decisions are assumed to be correct when the current symbol is estimated. The error auto-correlation matrix after CF linear detection is given by equality (24). It can be expanded as the difference of two terms: the first term is the error auto-correlation matrix after CNF linear detection, and the second term is a positive definite matrix given in equality (25).

An interesting property related to the Choleski decomposition is introduced.

Proposition 1: If $\boldsymbol{M}_a$, $\boldsymbol{M}_b$ and $\boldsymbol{M}_c$ are square positive definite matrices such that $\boldsymbol{M}_c = \boldsymbol{M}_a - \boldsymbol{M}_b$, they can be expanded according to Choleski as $\boldsymbol{M}_a = \boldsymbol{L}_a\boldsymbol{L}_a^H$, $\boldsymbol{M}_b = \boldsymbol{L}_b\boldsymbol{L}_b^H$ and $\boldsymbol{M}_c = \boldsymbol{L}_c\boldsymbol{L}_c^H$ where $\boldsymbol{L}_a$, $\boldsymbol{L}_b$ and $\boldsymbol{L}_c$ are lower triangular matrices with positive reals on the main diagonal. It can be proven that the diagonal elements of matrix $\boldsymbol{L}_c$ are always smaller than the diagonal elements of matrix $\boldsymbol{L}_a$. Proof: see Appendix A.

Assume that matrix $\boldsymbol{M}_c$ denotes the error auto-correlation matrix after a CF linear joint detector and $\boldsymbol{M}_a$ denotes the error auto-correlation matrix after a CNF linear joint detector. *Then the CF DF joint detector systematically outperforms the CNF DF joint detector since the error variances in case of CF sampling are given by the square of the diagonal elements of $\boldsymbol{L}_c$ and the error variances in case of CNF sampling are given by the square of the diagonal elements of $\boldsymbol{L}_a$.*

[2]If $\boldsymbol{X} = \boldsymbol{P}^{-1} + \boldsymbol{Q}\boldsymbol{T}^{-1}\boldsymbol{Q}^H$ where $\boldsymbol{X}$, $\boldsymbol{P}$, $\boldsymbol{T}$ are square positive-definite, then $\boldsymbol{X}^{-1} = \boldsymbol{P} - \boldsymbol{P}\boldsymbol{Q}\left(\boldsymbol{T}+\boldsymbol{Q}^H\boldsymbol{P}\boldsymbol{Q}\right)^{-1}\boldsymbol{Q}^H\boldsymbol{P}$.

IV. Continuous transmission

A. System decomposition

To be able to compare the CF and CNF detectors, the part of information which is available to the CNF detector is again isolated from the entirety of information. The same steps as in the burst transmission case are followed. Firstly, the receiver prefilter is separated in two parts. Secondly, a separation of even and odd samples is introduced. Definitions (2), (3) and (4) and the corresponding relation (5) are still valid.

We consider that the received signal is sampled at a CF rate and that each user transmits an infinite sequence of symbols. Furthermore we use a polyphase notation so that all sequences be defined at the same rate $1/T$. Please note that the sampling period common to the polyphase components was T_c in the case of burst transmission studied above. Based on the definitions (2), (3) and (4), let us define N_c polyphase components of each term as

$$r_\rho^i(n) \stackrel{def}{=} r^i(\rho+nN_c) \tag{27}$$

$$v_\rho^i(n) \stackrel{def}{=} v^i(\rho+nN_c) \tag{28}$$

$$g_{k,\rho}^{i,\gamma}(n) \stackrel{def}{=} g_k^{i,\gamma}(\rho+nN_c) \tag{29}$$

for $\rho = 0,\cdots,N_c-1$. In the z-domain, the initial model (1) becomes

$$r_\rho^i(z) = \sum_{k=1}^{K} d_k(z)\, g_{k,\rho}^{i,\alpha}(z) + \sum_{k=1}^{K} d_k(z)\, g_{k,\rho}^{i,\beta}(z) + v_\rho^i(z)$$

where $d_k(z)$, $r_\rho^i(z)$, $v_\rho^i(z)$ and $g_{k,\rho}^{i,\gamma}(z)$ are the z-transformed sequences $d_k(n)$, $r_\rho^i(n)$, $v_\rho^i(n)$ and $g_{k,\rho}^{i,\gamma}(n)$. The polyphase decomposition properties in [22] provide a counterpart of equality (29) in the frequency domain ($z = e^{j\Omega}$). If we define the vectors

$$\boldsymbol{\psi}_\rho^i(e^{j\Omega}) \stackrel{def}{=} \frac{1}{2N_c}\, e^{\frac{j(2\rho+i)\Omega}{2N_c}} \begin{bmatrix} 1 \\ e^{\frac{j2\pi(2\rho+i)}{2N_c}} \\ \vdots \\ e^{\frac{j2\pi(2\rho+i)(2N_c-1)}{2N_c}} \end{bmatrix} \tag{30}$$

and

$$\boldsymbol{g}_k^\gamma(e^{j\Omega}) \stackrel{def}{=} \begin{bmatrix} g_k^\gamma(e^{\frac{j\Omega}{2N_c}}) \\ g_k^\gamma(e^{\frac{j(\Omega+2\pi)}{2N_c}}) \\ \vdots \\ g_k^\gamma(e^{\frac{j(\Omega+2\pi(2N_c-1))}{2N_c}}) \end{bmatrix}, \tag{31}$$

we obtain

$$g_{k,\rho}^{i,\gamma}(e^{j\Omega}) = \left(\boldsymbol{\psi}_\rho^i(e^{j\Omega})\right)^T \boldsymbol{g}_k^\gamma(e^{j\Omega}) \tag{32}$$

by the use of property (5).

We define a vector of size $2N_c$ made of the N_c polyphase components corresponding to even and odd samples:

$$\boldsymbol{r}^{CF}(z) \stackrel{def}{=} \begin{bmatrix} \boldsymbol{r}^0(z) \\ \boldsymbol{r}^1(z) \end{bmatrix}$$

$$= \begin{bmatrix} \boldsymbol{G}^{0,\alpha}(z) + \boldsymbol{G}^{0,\beta}(z) \\ \boldsymbol{G}^{1,\alpha}(z) + \boldsymbol{G}^{1,\beta}(z) \end{bmatrix} \boldsymbol{d}(z) + \begin{bmatrix} \boldsymbol{v}^0(z) \\ \boldsymbol{v}^1(z) \end{bmatrix}$$
$$\stackrel{def}{=} \boldsymbol{G}^{CF}(z)\,\boldsymbol{d}(z) + \boldsymbol{v}^{CF}(z) \quad (33)$$

with

$$\boldsymbol{d}(z) \stackrel{def}{=} \begin{bmatrix} d_1(z) \\ \vdots \\ d_K(z) \end{bmatrix}$$
$$\boldsymbol{r}^i(z) \stackrel{def}{=} \begin{bmatrix} r_0^i(z) \\ \vdots \\ r_{N_c-1}^i(z) \end{bmatrix}$$
$$\boldsymbol{v}^i(z) \stackrel{def}{=} \begin{bmatrix} v_0^i(z) \\ \vdots \\ v_{N_c-1}^i(z) \end{bmatrix}$$

and

$$\boldsymbol{G}^{i,\gamma}(z) \stackrel{def}{=} \begin{bmatrix} G_{1,0}^{i,\gamma}(z) & \cdots & G_{K,0}^{i,\gamma}(z) \\ \vdots & \ddots & \vdots \\ G_{1,N_c-1}^{i,\gamma}(z) & \cdots & G_{K,N_c-1}^{i,\gamma}(z) \end{bmatrix}. \quad (34)$$

If the following matrices are defined based on definitions (30) and (31)

$$\boldsymbol{\Psi}^i(e^{j\Omega}) \stackrel{def}{=} \begin{bmatrix} \boldsymbol{\psi}_0^i(e^{j\Omega}) & \cdots & \boldsymbol{\psi}_{N_c-1}^i(e^{j\Omega}) \end{bmatrix} \quad (35)$$
$$\boldsymbol{G}^\gamma(e^{j\Omega}) \stackrel{def}{=} \begin{bmatrix} \boldsymbol{g}_1^\gamma(e^{j\Omega}) & \cdots & \boldsymbol{g}_K^\gamma(e^{j\Omega}) \end{bmatrix}, \quad (36)$$

definition (34) used together with (32) provides finally

$$\boldsymbol{G}^{i,\gamma}(e^{j\Omega}) = \left(\boldsymbol{\Psi}^i(e^{j\Omega})\right)^T \boldsymbol{G}^\gamma(e^{j\Omega}). \quad (37)$$

In case of CNF sampling ($M = 1$), the model becomes

$$\boldsymbol{r}^{CNF}(z) = \boldsymbol{G}^{CNF}(z)\,\boldsymbol{d}(z) + \boldsymbol{v}^{CNF}(z) \quad (38)$$

where $\boldsymbol{G}^{CNF}(z) = \boldsymbol{G}^{0,\alpha}(z)$.

B. Matrices expansion

If an AWGN is assumed, each performance measure (mutual information or error variance) for a continuous transmission is a function of $(\boldsymbol{G}^{CF}(e^{j\Omega}))^H \boldsymbol{G}^{CF}(e^{j\Omega})$ in the CF case and of $(\boldsymbol{G}^{CNF}(e^{j\Omega}))^H \boldsymbol{G}^{CNF}(e^{j\Omega})$ in the CNF case, with $\boldsymbol{G}^{CNF}(e^{j\Omega}) = \boldsymbol{G}^{0,\alpha}(e^{j\Omega})$.

About the CF case, we can write (see equation (33)):

$$\begin{aligned} &\left(\boldsymbol{G}^{CF}(e^{j\Omega})\right)^H \boldsymbol{G}^{CF}(e^{j\Omega}) \\ = \;& \left(\boldsymbol{G}^{0,\alpha}(e^{j\Omega})\right)^H \boldsymbol{G}^{0,\alpha}(e^{j\Omega}) + \left(\boldsymbol{G}^{1,\alpha}(e^{j\Omega})\right)^H \boldsymbol{G}^{1,\alpha}(e^{j\Omega}) \\ + \;& \left(\boldsymbol{G}^{0,\beta}(e^{j\Omega})\right)^H \boldsymbol{G}^{0,\beta}(e^{j\Omega}) + \left(\boldsymbol{G}^{1,\beta}(e^{j\Omega})\right)^H \boldsymbol{G}^{1,\beta}(e^{j\Omega}) \\ + \;& \left(\boldsymbol{G}^{0,\alpha}(e^{j\Omega})\right)^H \boldsymbol{G}^{0,\beta}(e^{j\Omega}) + \left(\boldsymbol{G}^{1,\alpha}(e^{j\Omega})\right)^H \boldsymbol{G}^{1,\beta}(e^{j\Omega}) \\ + \;& \left(\boldsymbol{G}^{0,\beta}(e^{j\Omega})\right)^H \boldsymbol{G}^{0,\alpha}(e^{j\Omega}) + \left(\boldsymbol{G}^{1,\beta}(e^{j\Omega})\right)^H \boldsymbol{G}^{1,\alpha}(e^{j\Omega}). \end{aligned} \quad (39)$$

Each term of expression (39) can be expanded using the relation (37), if we remark that [3]

$$\left(\boldsymbol{\Psi}^0(e^{j\Omega})\right)^H \boldsymbol{\Psi}^0(e^{j\Omega}) = \frac{1}{4N_c} \begin{bmatrix} \boldsymbol{I}_{N_c} & \boldsymbol{I}_{N_c} \\ \boldsymbol{I}_{N_c} & \boldsymbol{I}_{N_c} \end{bmatrix} \quad (40)$$
$$\left(\boldsymbol{\Psi}^1(e^{j\Omega})\right)^H \boldsymbol{\Psi}^1(e^{j\Omega}) = \frac{1}{4N_c} \begin{bmatrix} \boldsymbol{I}_{N_c} & -\boldsymbol{I}_{N_c} \\ -\boldsymbol{I}_{N_c} & \boldsymbol{I}_{N_c} \end{bmatrix} \quad (41)$$

where $\boldsymbol{I}_{N_c}$ is an identity matrix of size N_c. The different terms can be combined. We only provide the result for the sake of conciseness. Finally, we find

$$\left(\boldsymbol{G}^{CF}(e^{j\Omega})\right)^H \boldsymbol{G}^{CF}(e^{j\Omega}) = 2\left[\left(\boldsymbol{G}^{0,\alpha}(e^{j\Omega})\right)^H \boldsymbol{G}^{0,\alpha}(e^{j\Omega}) + \left(\boldsymbol{G}^{1,\alpha}(e^{j\Omega})\right)^H \boldsymbol{G}^{1,\alpha}(e^{j\Omega})\right]. \quad (42)$$

The first term corresponds to the CNF detector and the second term is the additional term corresponding to CF sampling. Remember that the noise variance in case of CF joint detector $(\sigma_v^{CF})^2$ is twice the noise variance in case of CNF joint detector $(\sigma_v^{CNF})^2$. This is due to the different bandwidths of the receiver presampling filters.

In the following sections, notation $\boldsymbol{S}_{xy}(z)$ stands for the cross-spectrum between $\boldsymbol{x}(z)$ and $\boldsymbol{y}(z)$. It is defined as the z-transformed cross-correlation matrix $\boldsymbol{R}_{xy}(n) = E\left[\boldsymbol{x}(m+n)\boldsymbol{y}^H(m)\right]$. Note that $\boldsymbol{x}(z)$ and $\boldsymbol{y}(z)$ are the z-transformed vectors $\boldsymbol{x}(n)$ and $\boldsymbol{y}(n)$. We introduce the following definitions

$$\boldsymbol{P}(z) \stackrel{def}{=} \left[\boldsymbol{S}_{dd}^{-1}(z) + \frac{1}{(\sigma_v^{CNF})^2}\left(\boldsymbol{G}^{0,\alpha}(1/z^*)\right)^H \boldsymbol{G}^{0,\alpha}(z)\right]^{-1} \quad (43)$$
$$\boldsymbol{Q}(z) \stackrel{def}{=} \left(\boldsymbol{G}^{0,\beta}(1/z^*)\right)^H \quad (44)$$
$$\boldsymbol{T}(z) \stackrel{def}{=} (\sigma_v^{CNF})^2\,\boldsymbol{I}_{N_c} \quad (45)$$

in order to simplify the notations in sections IV-C, IV-D and IV-E.

C. Mutual information

If an AWGN of variance $(\sigma_v^{CF})^2$ and Gaussian independent symbols of variance σ_d^2 are assumed, the mutual information between the infinite sequence of emitted symbols and the received sequence is given, in the CF case, by

$$I(\boldsymbol{d};\boldsymbol{r}^{CF}) = \frac{1}{2\pi}\int_{-\pi}^{\pi} \log\left|\boldsymbol{I}_K + \frac{\sigma_d^2}{(\sigma_v^{CF})^2}(\boldsymbol{G}^{CF}(e^{j\Omega}))^H \boldsymbol{G}^{CF}(e^{j\Omega})\right| d\Omega \quad (46)$$

$$= I(\boldsymbol{d};\boldsymbol{r}^{CNF}) + \frac{1}{2\pi}\int_{-\pi}^{\pi} \log\left|\boldsymbol{I}_K + \frac{1}{(\sigma_v^{CNF})^2}\boldsymbol{P}(e^{j\Omega})\boldsymbol{Q}(e^{j\Omega})(\boldsymbol{Q}(e^{j\Omega}))^H\right| d\Omega \quad (47)$$

[3] Remember that $\frac{1}{N}\sum_{l=0}^{N-1} e^{\frac{j2\pi ln}{N}} = \begin{cases} 1 \text{ if n is multiple of N} \\ 0 \text{ else} \end{cases}$.

Equality (46) gives the mutual information between an infinite sequence of emitted symbols and the received sequence. The capacity region of Gaussian linear multiple access channels with finite ISI has been computed in [16]. It gives the counterpart of the water-filling formula for multi-user channels. However the results of Verdu do not take into account the excess bandwidth inherent to a system using a DS-CDMA scheme (for example see equality (9) of [16] which is the same result as equality (46) for a system without excess bandwidth). In paper [17] the results of [16] are extended to systems with excess bandwidth. Starting from the classical result (21) and assuming that an infinite number of symbols is transmitted in the burst, equality (46) is found by the use of the asymptotic properties of Toeplitz matrices. Equality (47) comes from the decomposition (42) and from the fact that the noise variance in case of CF sampling is twice the noise variance in case of CNF sampling. The definitions (43) and (44) are also used. As $\boldsymbol{G}^{CNF}(e^{j\Omega}) = \boldsymbol{G}^{0,\alpha}(e^{j\Omega})$, the mutual information in the CNF case appears in equality (47).

The determinant of a matrix can be computed by the product of its eigen-values.
Matrix $\boldsymbol{P}(e^{j\Omega})\,\boldsymbol{Q}(e^{j\Omega})\,(\boldsymbol{Q}(e^{j\Omega}))^H$ is positive definite for any value of Ω. Its eigen-values are positive so that the eigen-values of $\boldsymbol{I}_{KN} + \frac{\sigma_d^2}{(\sigma_v^{CNF})^2}\boldsymbol{P}(e^{j\Omega})\,\boldsymbol{Q}(e^{j\Omega})\,(\boldsymbol{Q}(e^{j\Omega}))^H$ are larger than "1". It follows that the mutual information is always larger in the CF case. In Appendix B, equality (47) is particularized for a single-user system in order to be able to provide additional insight into the mutual information loss due to CNF sampling.

D. Linear MMSE joint detector

It will be demonstrated that the error variances of symbol estimates after CF linear MMSE JD are always smaller than those corresponding to the CNF one. The error cross-spectrum at the output of the CF detector is (an AWGN of variance $(\sigma_v^{CF})^2$ is assumed),

$$\begin{aligned} & \boldsymbol{S}_{\varepsilon\varepsilon}^{CF}(e^{j\Omega}) \\ = \;& [\boldsymbol{S}_{dd}^{-1}(e^{j\Omega}) + \frac{1}{(\sigma_v^{CF})^2}\,(\boldsymbol{G}^{CF}(e^{j\Omega}))^H\,\boldsymbol{G}^{CF}(e^{j\Omega})]^{-1} \qquad (48) \\ = \;& \boldsymbol{S}_{\varepsilon\varepsilon}^{CNF}(e^{j\Omega}) - \boldsymbol{S}_{\varepsilon\varepsilon}^{\beta}(e^{j\Omega}) \qquad (49) \end{aligned}$$

where

$$\begin{aligned} \boldsymbol{S}_{\varepsilon\varepsilon}^{\beta}(e^{j\Omega}) \stackrel{def}{=} \;& \boldsymbol{P}(e^{j\Omega})\,\boldsymbol{Q}(e^{j\Omega}) \\ & \left(\boldsymbol{T}(e^{j\Omega}) + (\boldsymbol{Q}(e^{j\Omega}))^H\,\boldsymbol{P}(e^{j\Omega})\,\boldsymbol{Q}(e^{j\Omega})\right)^{-1} \\ & \boldsymbol{Q}^H(e^{j\Omega})\,\boldsymbol{P}(e^{j\Omega}). \end{aligned}$$

Equality (48) is the classical expression of the error cross-spectrum matrix after linear MMSE JD [8, 11]. Equality (49) is obtained by using (42) and the fact that the noise variance in the CF case is twice the noise variance in the CNF case. The definitions (43), (44) and (45) are also used. Remember that $\boldsymbol{G}^{CNF}(e^{j\Omega}) = \boldsymbol{G}^{0,\alpha}(e^{j\Omega})$ so that the CNF error cross-spectrum matrix appears.

It can be easily proven that the matrix constituting the second term of (49) is positive definite for each frequency Ω so that its diagonal elements are positive reals. The error variances of symbol estimates are given by the diagonal terms of the zero order matrix coming from the integration of the error cross-spectrum on the unit circle ($z = e^{j\Omega}$). They are thus always smaller in the CF case.

E. Decision feedback MMSE joint detector

In case of DF JD, the geometrical mean of estimation error variances can be computed by using the fact that [8,12] (see especially equality (18) in [12])

$$\log \prod_i [\boldsymbol{R}_{\varepsilon\varepsilon}(0)]_{ii} = \frac{1}{2\pi}\cdot \int_{-\pi}^{\pi} \log \left| \left[\boldsymbol{S}_{dd}^{-1}(e^{j\Omega}) + \boldsymbol{G}^H(e^{j\Omega})\,\boldsymbol{S}_{vv}^{-1}(e^{j\Omega})\,\boldsymbol{G}(e^{j\Omega})\right]^{-1} \right| d\Omega$$

where $\boldsymbol{G}(e^{j\Omega})$ stands for $\boldsymbol{G}^{CNF}(e^{j\Omega})$ in the CNF case and for $\boldsymbol{G}^{CF}(e^{j\Omega})$ in the CF case.

The error cross-spectrum after linear JD is integrated on the unit circle. In the linear CF case, the error cross-spectrum (expression (48)) can be decomposed in two terms, each constituted of positive definite matrices for any value of Ω (see equality (49)). Furthermore, the first term corresponds to the error cross-spectrum in the CNF case. A Choleski decomposition can be applied to each part for a given Ω. The determinant is equal to the products of the diagonal elements coming from the Choleski decomposition matrices since those matrices are triangular. By means of Proposition 1 about the Choleski decomposition, it is easily proven that the geometrical mean of errors is always smaller in the CF case.

V. Results

The purpose of this section is to compare numerically three different receiver configurations. In the previous sections, we have assumed that an ideal LP filter is applied on the received signal in order to avoid aliasing. In this case, the signal is sampled at either a CF or a CNF rate. We have demonstrated that CF sampling outperforms always the CNF one. This will be confirmed by computational results. We consider also a system where a chip MF is applied on the received signal before CNF sampling. This last configuration will be compared to the two previous ones.

For mobile communications, the channels can be modeled as multi-path channels. In this paper, we have assumed four-path channels. The amplitudes and the phases are chosen arbitrarily. The delays are given in fractions of the chip duration. For the computations, the channel delay spread (which is defined as the maximal path delay) is equal to 0.9 μs. A system composed of 16 users, each of them sending a burst of 10 symbols, is considered. The chip duration T_c is equal to 0.25 μs. Gold codes of length 31 are used to spread the symbols of the different users. The spreading factor N_c is equal to 31. A half-root Nyquist filter, characterized by a roll-off factor equal to 0.3, is used to

shape the emitted signals. The ratio E_s/N_0, where E_s denotes the received symbol energy and N_0 denotes the noise one-sided power spectral density equal to -100 dBm/Hz, is fixed to 20 dB. A perfect power control for each user is assumed. The sampling phase is chosen to be aligned with the first path, which we expect to be a favorable situation for the CNF detector.

Table I gives the mutual information between the emitted sequences of symbols and the received sequence, and the geometrical mean of the user signal to interference and noise ratios (SINRs, see paper [10] for a close definition) for the set of parameters considered above. In case of CNF sampling, a little part of the information contained in the received signal is removed by the ideal LP filter. Furthermore, the computational results show that the mutual information is smaller if a chip MF is applied instead of an ideal LP filter. The same conclusions hold for the different user SINRs after a linear or DF MMSE joint detector. Figure 4 illustrates the user SINRs after a linear or DF MMSE joint detector. Each separate user SINR is the geometrical mean of the SINRs corresponding to the different symbols of that user in the emitted burst. In case of linear JD, all user symbols are detected simultaneously. In case of DF JD, we consider that the symbols are detected following either the symbol index order or the inverted symbol index order. The SINRs corresponding to the lastly detected users are close to the matched filter bound equal to 20 dB since the interference due to the previously detected users is removed from the received signal. Each separate user performance gain between the three possible configurations varies according to the user detection order. However it can be easily demonstrated that the geometrical mean of all user symbol SINRs is constant. Comparing CF and CNF sampling, gains up to 1.26 dB and up to 1.11 dB are observed for user 5 for the CF linear and DF MMSE joint detectors respectively.

Figure 5 shows the mutual information between the emitted symbols and the received sequence as a function of the roll-off factor. Of course, the mutual information is the same for all receivers if the roll-off factor is equal to 0. For higher values, the curves move away from each other. When the roll-off factor becomes higher, the ideal LP filter applied before the CNF sampling removes an increasing amount of the signal received energy. A gain up to 0.2 bits per emitted symbol is observed between the CF and CNF sampling rates. Figures 6 and 7 show the geometrical mean of the user SNIRs after linear and DF MMSE JD as a function of the roll-off factor. Regarding CF and CNF receivers, gains up to 1 dB and 0.7 dB are observed for the CF linear and DF MMSE joint detectors.

The ultimate performance criterion is the bit error probability. Regarding the different users and receivers, it should be interesting to link the performance metrics considered in the analytical derivations (the mutual information and the mean square errors) with the corresponding bit error probabilities. The performance of users 5 and 14 is investigated by performing simulations for E_s/N_0 ratios ranging from 0 to 14 dB and for a quadrature phase shift keying (QPSK) modulation. At least 1000 errors on the bit decisions have been detected for each user. Figures 8 and 9 illustrate the bit error rates (BERs) at the output of the linear and DF MMSE joint detectors. It is well known that the DF MMSE joint detector suffers from symbol detection error propagation mechanisms. In Figure 10, the performance of the actual DF MMSE joint detector is compared to the performance obtained when perfect decisions on the previous symbols are assumed. Only the case of CF sampling after an ideal LP filter has been considered for the last comparison. The performance is improved when the symbols are correctly detected. However the curves are shown to converge to each other for low bit error rates. Traditionally, the bit error probabilities are theoretically computed based on the different user SINRs by supposing that the interference at the output of the joint detector is Gaussian. The related curves are also illustrated in Figures 8 and 10 for the linear and DF MMSE joint detectors respectively. In the linear case, the values match perfectly the simulations. In the DF case, the values are close to the values obtained with a perfect feedback. Hence there is a good match between the different metrics. CF sampling at the output of an ideal LP filter is shown to outperform significantly CNF sampling. A system using CNF sampling after a chip MF still offers a lower performance.

VI. Conclusion

This paper compares the performance of CF and CNF sampling at the receiver for a CDMA uplink transmission. It is analytically shown that CF sampling always outperforms CNF sampling and an expression of the gain in performance is provided. Firstly, the mutual information between the emitted sequences of symbols and the received sequence is investigated. A difference of 0.1 bits per emitted symbol arises for the setup used here, that is multi-path channels and a 0.3 roll-off factor. Secondly, the error variances of the symbol estimates after linear and DF MMSE JD are discussed. Considering the geometrical mean of the different user SINRs separately in case of linear and DF JD, a gain up to 1.26 dB and 1.11 dB respectively arises for the same classical value of the roll-off factor. The choice between CF and CNF sampling has obviously an impact on the system complexity. In the CF case, the computation cost for the detection would be twice that for CNF. This has to be taken into account for a global assessment.

In practice, the channels have to be estimated, and the joint detectors are deduced from estimated channels. Further work will include the study of the degradation due to the estimation of the different impulse responses.

Appendix A

Proof of Proposition 1: By the use of the definition, we have $\boldsymbol{L}_a \boldsymbol{L}_a^H = \boldsymbol{L}_b \boldsymbol{L}_b^H + \boldsymbol{L}_c \boldsymbol{L}_c^H$. Matrix $\boldsymbol{L}_a$ is invertible, and thus, $\boldsymbol{L}_a^{-1} \left(\boldsymbol{L}_b \boldsymbol{L}_b^H + \boldsymbol{L}_c \boldsymbol{L}_c^H \right) \left(\boldsymbol{L}_a^H \right)^{-1} = \boldsymbol{I}$ where $\boldsymbol{I}$ is the identity matrix. If we define the two modified lower triangular matrices $\hat{\boldsymbol{L}}_b = \boldsymbol{L}_a^{-1} \boldsymbol{L}_b$ and $\hat{\boldsymbol{L}}_c = \boldsymbol{L}_a^{-1} \boldsymbol{L}_c$, the

last expression becomes $\hat{\boldsymbol{L}}_b \hat{\boldsymbol{L}}_b^H + \hat{\boldsymbol{L}}_c \hat{\boldsymbol{L}}_c^H = \boldsymbol{I}$. The development of the diagonal element p of each part gives

$$\sum_{q=1}^{p} [\hat{\boldsymbol{L}}_b]_{pq}^* [\hat{\boldsymbol{L}}_b]_{pq} + \sum_{q=1}^{p} [\hat{\boldsymbol{L}}_c]_{pq}^* [\hat{\boldsymbol{L}}_c]_{pq} = 1$$

The diagonal elements of $\hat{\boldsymbol{L}}_c$ are thus always smaller than 1. The matrices $\boldsymbol{L}_a$ and $\boldsymbol{L}_c$ are lower triangular matrices. Hence, it can be easily demonstrated that $[\boldsymbol{L}_a^{-1}]_{pp} [\boldsymbol{L}_c]_{pp} \leq 1$ using the definition of $\hat{\boldsymbol{L}}_c$. Furthermore, we have that $[\boldsymbol{L}_a^{-1}]_{pp} [\boldsymbol{L}_a]_{pp} = 1$ so that the diagonal elements of $\boldsymbol{L}_c$ are always smaller than or equal to the diagonal elements of $\boldsymbol{L}_a$. *QED*

Appendix B

If CF sampling is considered, the sequence of samples contains all the received signal information. However, in case of CNF sampling, the LP receiver prefilter removes a part of the information in order to avoid aliasing. Equality (47) gives the expression of the mutual information loss in case of continuous transmission. If only one user is considered in the system, it is possible to give more insight into this last result. By introducing definitions (43) and (44) in equality (47), and by using property (5), the mutual information loss is

$$\frac{1}{\pi} \int_{-\pi/2}^{-\pi/2} \log \left(1 + \frac{\sigma_d^2 G^\beta(e^{j(\Omega-\pi)})^* G^\beta(e^{j(\Omega-\pi)})}{4(\sigma_v^{CNF})^2 + \sigma_d^2 G^\alpha(e^{j\Omega})^* G^\alpha(e^{j\Omega})} \right) d\Omega \tag{50}$$

in the single user case. The term $G^\alpha(e^{j\Omega})^* G^\alpha(e^{j\Omega})$ corresponds to the signal received energy located in the Nyquist zone (frequencies between $-0.5/T_c$ and $0.5/T_c$). The term $G^\beta(e^{j(\Omega-\pi)})^* G^\beta(e^{j(\Omega-\pi)})$ corresponds to the signal received energy located in the excess bandwidth and shifted to the Nyquist zone.

If the system works without excess bandwidth, CNF sampling is sufficient to keep the whole information contained in the received signal. When the roll-off factor increases, the loss of information due to CNF sampling becomes higher. It is noteworthy that the information loss depends not only on the information located in the excess bandwidth but also on the initial information located in the Nyquist zone. The signal located in the excess bandwidth brings redundancy as compared to the signal located in the Nyquist zone. In other words it is the same source which is "hidden" behind the information carried by the two bands. Therefore the information do not just add together. Hence if the information contained in the Nyquist zone is high, the information brought by the excess bandwidth is less important.

References

[1] C.E. Shannon, "Communications in the Presence of Noise", *Proc. IRE*, vol. 37, 1949, pp. 10-21.

[2] H. Meyr, M. Oerder, A. Polydoros, "On Sampling Rate, Analog Prefiltering, and Sufficient Statistics for Digital Receivers", *IEEE Transactions on Communications*, vol. 42, No. 12, December 1994, pp. 3208-3214.

[3] J.R. Treichler, I. Fijalkow, C.R. Johnson, "Fractionally Spaced Equalizers", *IEEE Signal Processing Magazine*, vol. 13, May 1996, pp. 65-81.

[4] R.D. Gitlin, S.B. Weinstein, "Fractionally-Spaced Equalization: An Improved Digital Transversal Equalizer", *The Bell System Technical Journal*, vol. 60, No. 2, February 1981, pp. 275-296.

[5] D.R. Brown, D.L. Anair, C.R. Johnson, "Fractionally Sampled Linear Detectors for DS-CDMA", *Proceedings of the 33rd Asilomar Conference on Signals, Systems and Computers*, Pacific Grove, CA, November 1998.

[6] S. Verdu, "Minimum Probability of Error for Asynchronous Gaussian Multiple-Access Channels", *IEEE Transactions on Information Theory*, vol. 32, No. 1, January 1986, pp. 85-96.

[7] R. Lupas, S. Verdu, "Linear Multiuser Detectors for Synchronous Code-Division Multiple-Access Channels", *IEEE Transactions on Information Theory*, vol. 35, No. 1, January 1989, pp. 123-136.

[8] A. Duel-Hallen, "Equalizers for Multiple Input/Multiple Output Channels and PAM Systems with Cyclostationary Input Sequences", *IEEE Journal on Selected Areas in Communications*, vol. 10, No. 3, April 1992, pp. 630-639.

[9] A. Duel-Hallen, "A family of multi-user decision-feedback detectors for asynchronous CDMA channels", *IEEE Transactions on Communications*, vol. 43, No. 3, April 1995, pp. 421-434.

[10] J. M. Cioffi, G. P. Dudevoir, M. V. Eyuboglu, G. D. Forney, "MMSE Decision-Feedback Equalizers and Coding - Part 1: Equalization Results", *IEEE Transactions on Communications*, vol. 43, No. 10, October 1995, pp. 2582-2594.

[11] L. Vandendorpe, "Performance analysis of IIR and FIR linear and decision-feedback MIMO equalizers for transmultiplexers", *Proc. ICC 97*, Monreal, Canada, June 1997, pp. 657-661.

[12] L. Vandendorpe, J. Louveaux, B. Maison, A. Chevreuil, "About the Asymptotic Performance of MMSE MIMO DFE for Filter-Bank Based Multicarrier Transmission", *IEEE Transactions on Communications*, vol. 47, No. 10, October 1999, pp. 1472-1475.

[13] A. Klein and P.W. Baier, "Linear Unbiased Data Estimation in Mobile Radio Systems Applying CDMA", *IEEE Journal on Selected Areas in Communications*, vol. 11, No. 7, September 1993, pp. 1058-1066.

[14] A. Klein, G.K. Kaleh and P.W. Baier, "Zero Forcing and Minimum Mean Square Error Equalization for Multiuser Detection in Code Division Multiple Access Channels", *IEEE Transactions on Vehicular Technology*, vol. 45, No. 2, May 1996, pp. 276-287.

[15] Naofal Al-Dhahir, John M. Cioffi, "Block Transmission over Dispersive Channels: Transmit Filter Optimization and Realization, and MMSE-DFE Receiver Performance", *IEEE Transactions on Information Theory*, vol. 42, No. 1, January 1996, pp. 137-160.

[16] R.S. Cheng, S. Verdu, "Gaussian Multiaccess Channels with ISI: Capacity Region and Multiuser Water-Filling", *IEEE Transactions on Information Theory*, vol. 39, No. 3, May 1993, pp. 773-785.

[17] F. Horlin, L. Vandendorpe, "Burst and continuous transmission for DS-CDMA uplink communication: performance study and comparison", *submitted to IEEE Transactions on Communication.*

[18] "CDMA: Principles of Spread Spectrum Communication", Andrew J. Viterbi, Addison-Wesley Wireless Communications Series, Massachusetts, 1995.

[19] "Multi-User Detection", Sergio Verdu, Press syndicate of the university of Cambridge, 1998.

[20] "Digital Communications", J.G. Proakis, Mc Graw-Hill International Editions, Third Edition, 1995.

[21] "Digital Communication Receiver", Heinrich Meyr, Marc Moeneclaey, Stephan A. Fechtel, Wiley Series in Telecommunications and Signal Processing, New York, 1998.

[22] "Multirate systems and filter banks", P.P. Vaidyanathan, Prentice Hall Signal Processing Series, 1993.

[23] "Introduction to matrix analysis", R. Bellman, Mc Graw-Hill, 1960.

[24] "Stationary random processes", Y.A. Rozanov, Holden-Day, 1967.

[25] "Matrix computations", G.H. Golub, C.F. Van Loan, North Oxford Academic, Oxford, 1983.

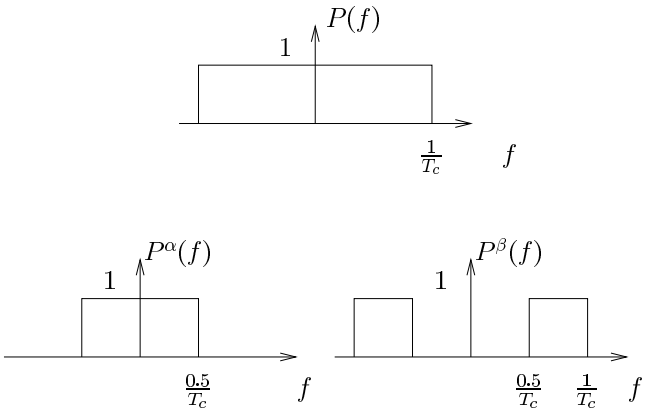

Fig. 2. Prefilter decomposition

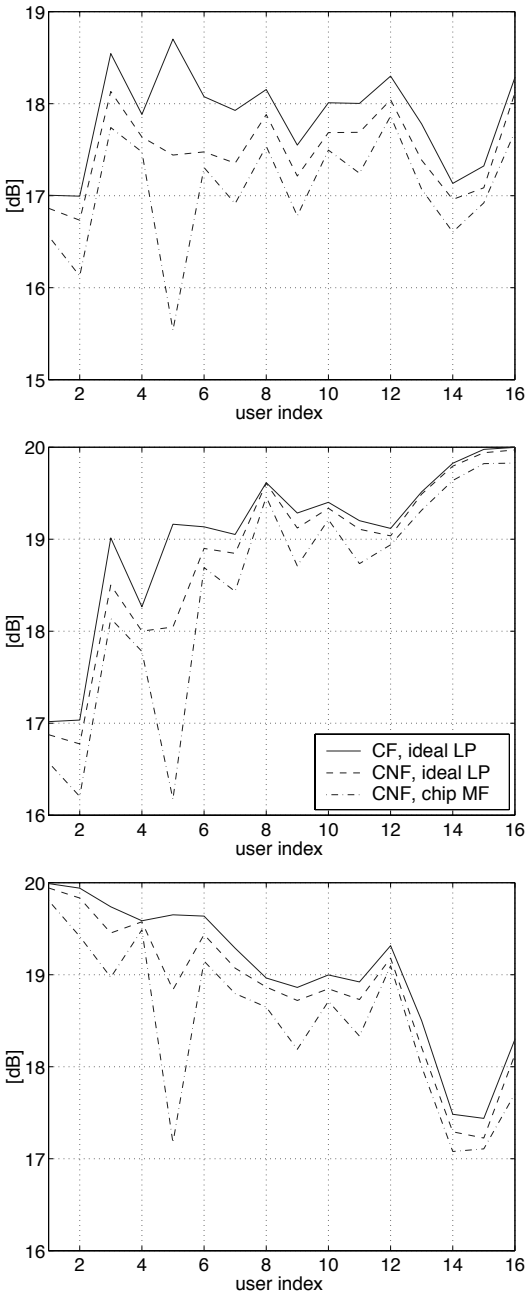

Fig. 4. (A) Geometrical mean of each user SINRs after a linear joint detector. (B) Geometrical mean of each user SINRs after a DF joint detector. (C) Geometrical mean of each user SINRs after a DF joint detector assuming an inverted symbol detection order.

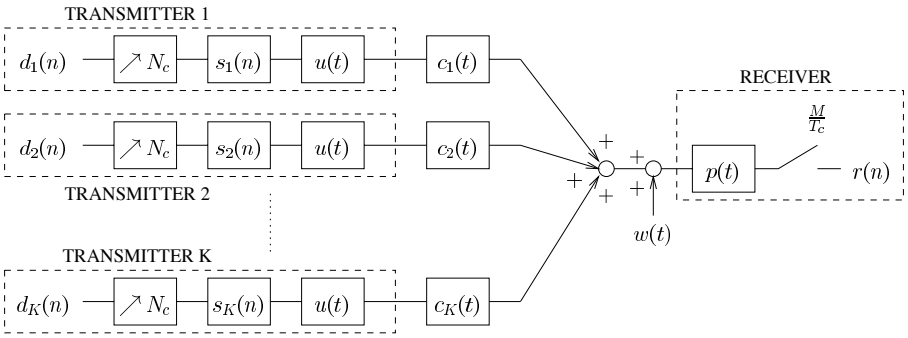

Fig. 1. System model

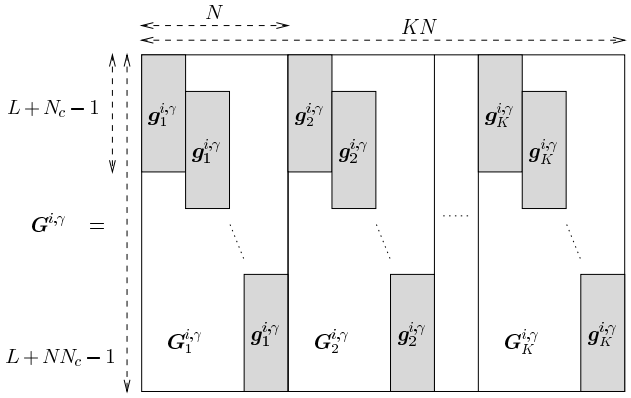

Fig. 3. Total impulse response matrix

	CF, ideal LP	CNF, ideal LP	CNF, chip MF
Mutual information [bits/symbol]	6.35	6.28	6.16
MMSE linear [dB]	17.85	17.48	17.05
MMSE DF [dB]	19.04	18.83	18.48

TABLE I

MUTUAL INFORMATION BETWEEN THE EMITTED SEQUENCES OF SYMBOLS AND THE RECEIVED SEQUENCE. GEOMETRICAL MEAN OF THE USER SINRS IN CASE OF LINEAR AND DF JOINT DETECTORS.

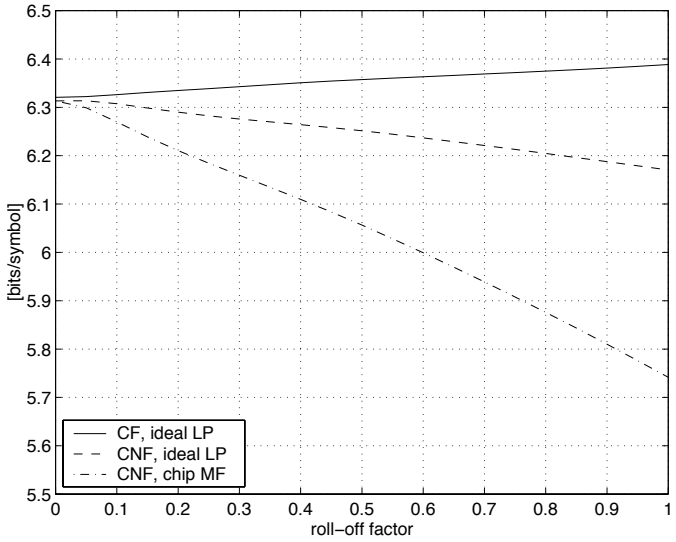

Fig. 5. Mutual information between the emitted sequences of symbols and the received sequence as a function of the roll-off factor.

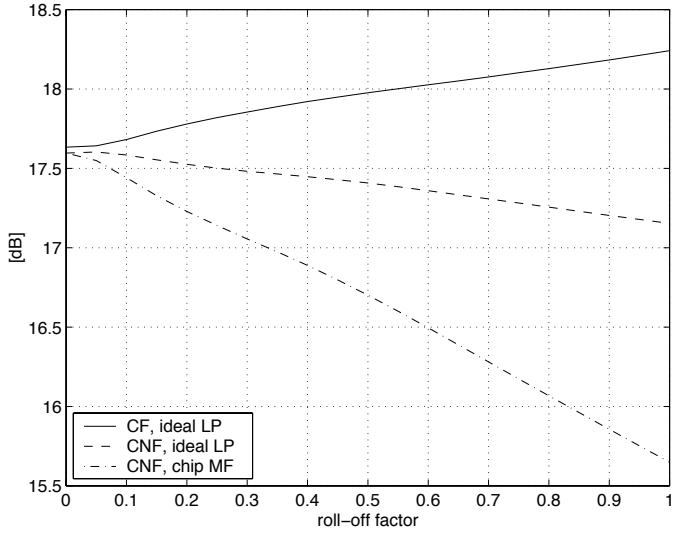

Fig. 6. Geometrical mean of SINRs after a linear MMSE joint detector as a function of the roll-off factor.

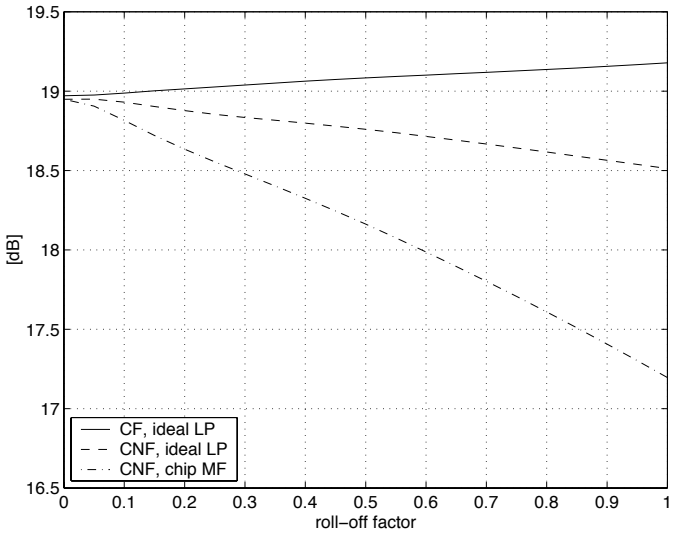

Fig. 7. Geometrical mean of SINRs after a DF MMSE joint detector as a function of the roll-off factor.

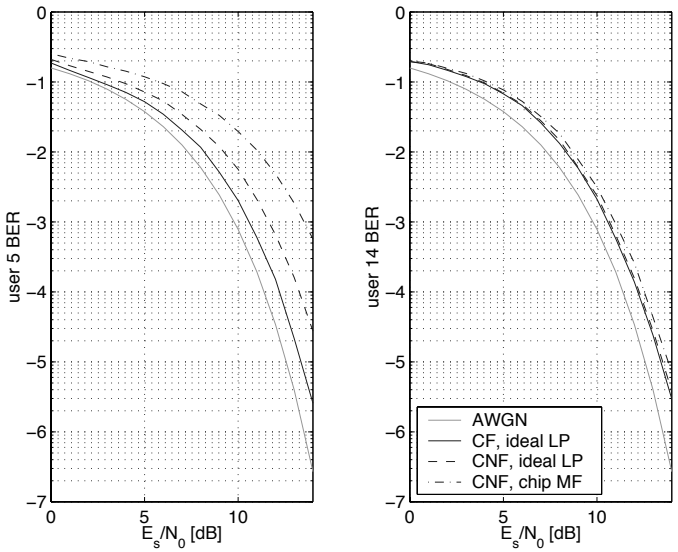

Fig. 9. Users 5 and 14 BERs at the output of the DF MMSE joint detector.

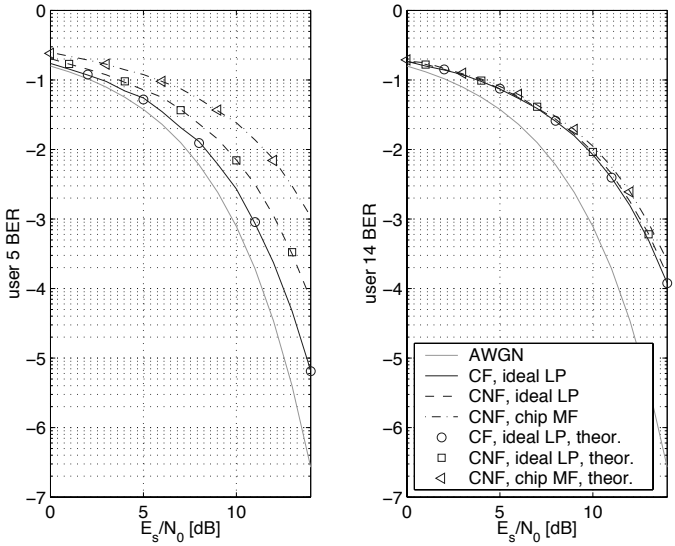

Fig. 8. Users 5 and 14 BERs at the output of the linear MMSE joint detector. Comparison between the actual values and the theoretical values obtained assuming a Gaussian interference.

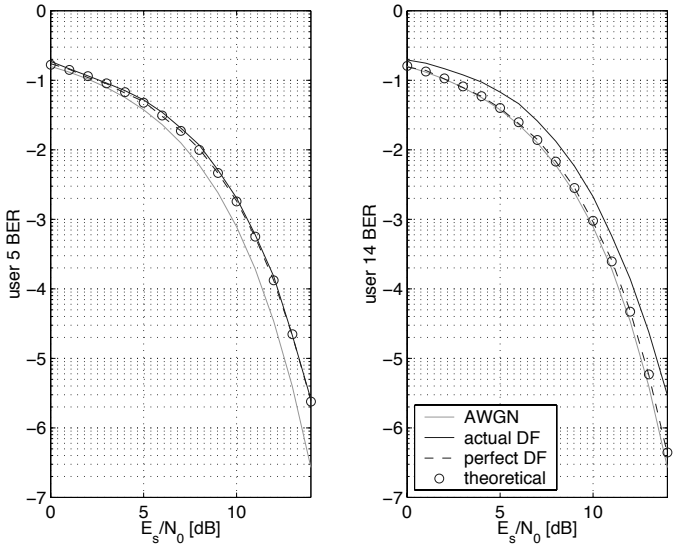

Fig. 10. Users 5 and 14 BERs at the output of the DF MMSE joint detector working at a CF rate. Comparison between the actual DF JD performance, the DF JD performance assuming perfect previous symbol decisions and the theoretical performance obtained assuming a Gaussian interference.